The Astrophysical Journal Letters, 812:L31 (5pp), 2015 October 20 doi:10.1088/2041-8205/812/2/L31

A HOT HORIZONTAL BRANCH STAR WITH A CLOSE K-TYPE MAIN-SEQUENCE COMPANION*

C. Moni Bidin[1], Y. Momany[2], M. Montalto[3], M. Catelan[4,5], S. Villanova[6], G. Piotto[2,7], and D. Geisler[6]
[1] Instituto de Astronomía, Universidad Católica del Norte, Av. Angamos, 0610, Antofagasta, Chile; cmoni@ucn.cl
[2] Istituto Nazionale di Astrofisica—Osservatorio Astronomico di Padova, Vicolo dell'Osservatorio 5, I-35122 Padova, Italy
[3] Instituto de Astrofísica e Ciências de Espaço, Universidade do Porto, Rua das Estrelas, PT 4150-762, Porto, Portugal
[4] Instituto de Astrofísica, Pontificia Universidad Católica de Chile, Casilla 306, Santiago, Chile
[5] Millennium Institute of Astrophysics, Santiago, Chile
[6] Departamento de Astronomía, Universidad de Concepción, Casilla 160-C, Concepción, Chile
[7] Dipartimento di Fisica e Astronomia "Galileo Galilei," Universitá di Padova, Vicolo dell'Osservatorio 3, Padova, I-35122 Padova, Italy
Received 2015 August 7; accepted 2015 September 23; published 2015 October 19

ABSTRACT

Dynamical interactions in binary systems are thought to play a major role in the formation of extreme horizontal branch stars (EHBs) in the Galactic field. However, it is still unclear if the same mechanisms are at work in globular clusters (GCs), where EHBs are predominantly single stars. Here, we report on the discovery of a unique close binary system (period ∼1.61 days) in the GC NGC 6752, comprising an EHB and a main-sequence companion of $0.63 \pm 0.05\ M_{\odot}$. Such a system has no counterpart among nearly 200 known EHB binaries in the Galactic field. Its discovery suggests that either field studies are incomplete, missing this type of system possibly because of selection effects, or that a particular EHB formation mechanism is active in clusters but not in the field.

Key words: binaries: close – stars: horizontal-branch – subdwarfs

1. INTRODUCTION

Extreme horizontal branch stars (EHBs) are hot ($T_{\rm eff} >$ 20,000 K), evolved stars of low initial mass (0.7–2 $M_{\odot}$) burning helium in their core (Faulkner 1972; Heber 1986). They have lost most of the hydrogen envelope during their evolution, to the point that the external layer is too thin to sustain the hydrogen-burning shell. Thus, after the exhaustion of helium, they are expected to evolve directly to the white dwarf cooling sequence ("AGB-manqué stars"; Greggio & Renzini 1990). They are found both in the Galactic field and in globular clusters (GCs), and the comprehension of their formation mechanisms is required to understand the late stages of the evolution of low-mass stars. They are also responsible for the ultraviolet emission of elliptical galaxies (Greggio & Renzini 1990; Han et al. 2007; Chung et al. 2011).

The causes of the heavy mass loss required to form an EHB star are still under debate, and this is one of the foremost gray areas of low-mass stellar evolution theory. Dynamical interactions inside binary systems are considered a major channel to produce an EHB star (Han et al. 2002, 2003), as confirmed by the high frequency of close binaries among EHBs in the Galactic field (e.g., Kawka et al. 2015). However, it is unclear if the same mechanisms are at work in the denser environment of GCs, where close EHB binaries are very rare (Moni Bidin et al. 2006, 2009). The old age of the cluster stellar population was proposed as an explanation (Han 2008; Moni Bidin et al. 2008), but an alternative scenario has become more popular in the last decade: EHBs could be the progeny of second-generation, single, helium-enriched stars (D'Antona et al. 2002; Chung et al. 2011; Dalessandro et al. 2011).

The star M5865 in NGC 6752 so far is the only spectroscopically confirmed EHB close binary in a GC (Moni Bidin et al. 2008). Later after discovery, Moni Bidin & Piotto (2010) showed that the presence of a G- or K-type main-sequence (MS) companion had previously been proposed for this star by Moni Bidin et al. (2007) to explain its red color and a faint MgIb triplet in its spectrum. An EHB star with a close companion of this kind has never been observed among the more than 180 EHB binaries discovered to date in the Galactic field (Østensen 2006; Wade et al. 2014). In fact, their close companions are all either compact remnants (white dwarfs or neutron stars) or very low-mass MS stars ($M_{\rm MS} < 0.3\ M_{\odot}$; e.g., Morales-Rueda et al. 2003; Maxted et al. 2011). More massive MS companions have been found only in wide pairs (e.g., Vos et al. 2013) or hierarchical triple systems (Heber et al. 2002). Indeed, M5865 could be such a rare triple system, where the MS star in a wide orbit does not interfere with the evolution of the inner, close pair. Alternatively, the MS star could also be a foreground object physically unrelated to the EHB star, a common fact in the crowded environment of GCs.

We analyzed the available data of M5865 to identify the role of the MS star in the system. The data sets consisted of (i) 21 high-resolution spectra, (ii) 5 intermediate-resolution spectra, (iii) composite ground-based optical images, (iv) and more than 800 frames of time-series photometry in the V band.

2. DATA ANALYSIS

2.1. The Mass of the MS Star

We estimated the mass of the MS star ($M_{\rm MS}$), comparing the position of the star in the color–magnitude diagram (CMD) to a synthetic loci representative of an EHB star plus an MS companion. We empirically determined the starting point of the curve, i.e., the position of a single cluster HB star ($(U-V)_{\rm EHB}$, $V_{\rm EHB}$) at the temperature of the hot component of the system ($T_{\rm eff,MS} = 27800 \pm 300$ K; Moni Bidin et al. 2007). We fitted a $(U-V)$–$T_{\rm eff}$ relation to the hotter part of the horizontal branch (HB) of NGC 6752, matching photometric colors (obtained with WFI at the MPG/ESO Telescope; Momany et al. 2002) with spectroscopic temperature measurements (Moni Bidin et al. 2007). We excluded all the stars with

* Based on observations with the ESO Very Large Telescope at Paranal Observatory, Chile (program IDs 69.D-0682, 075.D-0492, and 079.D-0674), and with the 6.5 m *Magellan* Telescopes at Las Campanas Observatory, Chile (program IDs 2006B-LC-7 and CHILE-2007B-007).

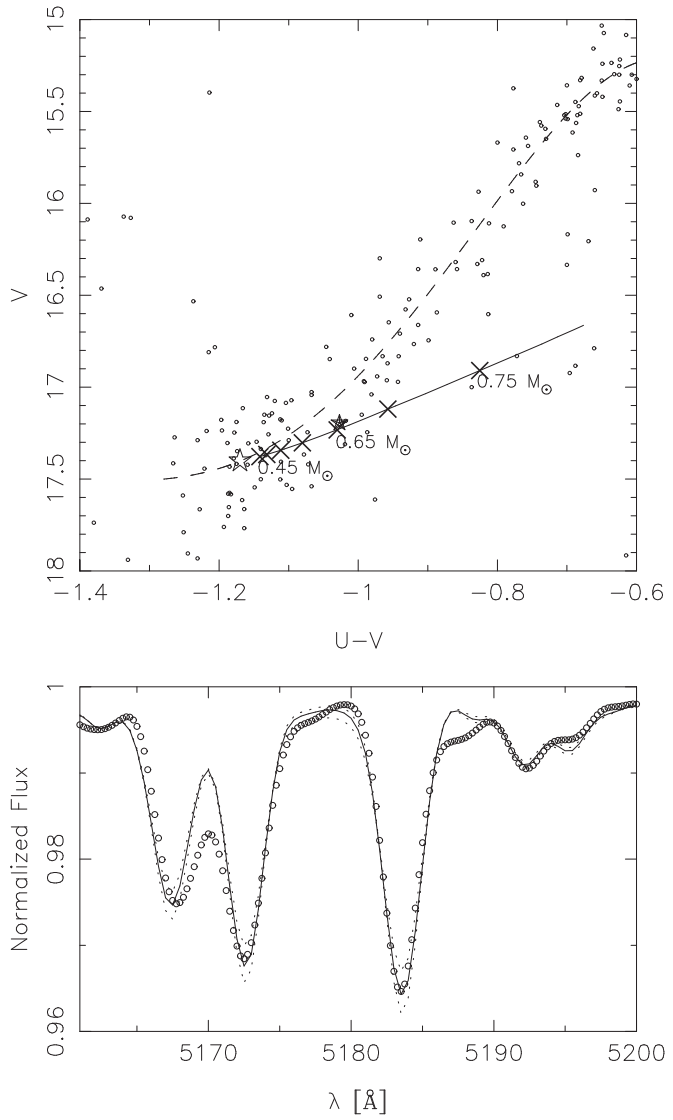

Figure 1. Upper panel: photometric mass estimate for the MS star. The filled and empty stars indicate the observed and theoretical (as a single star) position of M5865, respectively. Other cluster stars are shown with small circles, and the dashed curve indicates the polynomial fit of the cluster HB. Solid curve and crosses show the positions of an EHB star plus an MS star of increasing mass, from 0.45 to 0.78 $M_{\odot}$. Lower panel: spectroscopic mass estimate for the MS star. The observed MgIb triplet (empty circles) is compared to synthetic spectra of an EHB star with an MS companion of varying mass. The best-fit model ($T_{\rm eff,MS}$ = 5300 K) is indicated by the thick curve. The dashed curves show the same synthetic spectrum, with $T_{\rm eff,MS}$ varied by ±100 K.

"anomalous" spectroscopic results, in particular the eight EHBs with high spectroscopic mass, and we were left with 23 stars. We thus derived $(U-V)_{\rm EHB} = -1.18 \pm 0.03$. The error was estimated from the scatter of the points with respect to the fitted curve, as also done for the magnitude obtained in the next step. We then fitted a fourth-order polynomial to the HB in the CMD (dashed curve in Figure 1), and from the color $(U-V)_{\rm EHB}$ we derived $V_{\rm EHB} = 17.39 \pm 0.18$. Given the expected photometric properties of the EHB component alone, we calculated the magnitude and color when the flux of an MS star between $M_{\rm MS} = 0.45$ and 0.78 $M_{\odot}$ is added. This was taken from Yale-Yonsei theoretical isochrones (Spada et al. 2013) for metallicity $Z = 0.0004$ and age = 12.5 Gyr (VandenBerg et al. 2013), assuming $(m-M) = 13.38$, $E(B-V) = 0.04$ (Harris 1996), and a standard reddening law (Cardelli et al. 1989). We thus obtained the curve shown in Figure 1, with color and magnitude increasing with $M_{\rm MS}$. The point closest to the observed position returned $M_{\rm MS} = 0.64 \pm 0.07\ M_{\odot}$. The error was estimated from the variations of the result when the starting point was shifted by 1σ in either magnitude or color (assuming an error of 0.05 mag in distance modulus). The photometric error of the observed position was considered also, but it had negligible incidence on the result (0.006 and 0.012 mag in V and $(U-V)$, respectively).

The MgIb triplet, signature of the MS star, was observed in five intermediate-resolution ($R = 4000$) spectra collected with FORS2 at Paranal Observatory between 2002 June 11 and 14, with the 1400 V grism and a 0.″5 wide slit. We remand the reader to Moni Bidin et al. (2006) for more details about the observations and the data reduction. We obtained a spectroscopic estimate of $M_{\rm MS}$ by fitting this feature with synthetic spectra. We shifted the spectra to laboratory wavelength and co-added them. Flux-calibrated synthetic spectra were calculated with the SPECTRUM LTE spectral synthesis code (Gray & Corbally 1994), fed with model atmospheres obtained by interpolating on the Kurucz (1993) grid. The temperature and gravity of the EHB star were taken from our previous measurements (Moni Bidin et al. 2007). We calculated five models with $T_{\rm eff,MS}$ between 3800 and 5800 K, in steps of 500 K. Their gravities and masses were taken from the same models used before. We interpolated the three hottest models at a step of 100 K to produce a finer grid in the range $T_{\rm eff,MS}$ = 4800–5800 K. The stellar radii were estimated as $R = (MG/g)^{0.5}$, where g is the surface gravity and M is the mass, assuming 0.5 $M_{\odot}$ for the EHB star. We then scaled the fluxes for the different radii of the two components and co-added them. We compared each model with the observed spectrum, calculated the χ^2 statistics, and fitted its dependence on $T_{\rm eff,MS}$ with a third-order polynomial. We thus found a minimum χ^2 at $T_{\rm eff,MS} = 5310 \pm 140$ K, corresponding to an MS star with $M_{\rm MS} = 0.62 \pm 0.03\ M_{\odot}$. The fit is shown in Figure 1. The errors were estimated from the statistical behavior of the χ^2 function. They are likely underestimated because only random noise of the observed spectrum is taken into account, while systematic effects, such as errors in the continuum placement or the exact magnesium abundance, can occur.

The two independent approaches returned very similar results. Accounting for possible systematics, we derive $M_{\rm MS} = 0.63 \pm 0.05\ M_{\odot}$. According to the employed models, the cool star is therefore an early K-type MS object with $T_{\rm eff,MS} = 5310 \pm 20$ K and $V_{\rm MS} = 19.6 \pm 0.1$.

2.2. Orbital Solution of the EHB

Seventeen high-resolution ($R = 18{,}000$) spectra centered on the H_{β} line were collected between 2007 June and September in service mode at Paranal Observatory, with the FLAMES-GIRAFFE spectrograph and the H7A setup. This data set was complemented with four more epochs, collected on 2005 June 29, with the same instrument and setup (Moni Bidin et al. 2008). We reduced the data by means of the CPL-based ESO pipeline. We checked the wavelength calibration analyzing the extracted and calibrated lamp fibers, and we found only small random deviations from the laboratory wavelengths (0.3 km s^{-1} rms). We extracted the science spectra with an optimum algorithm (Horne 1986) and subtracted the smoothed

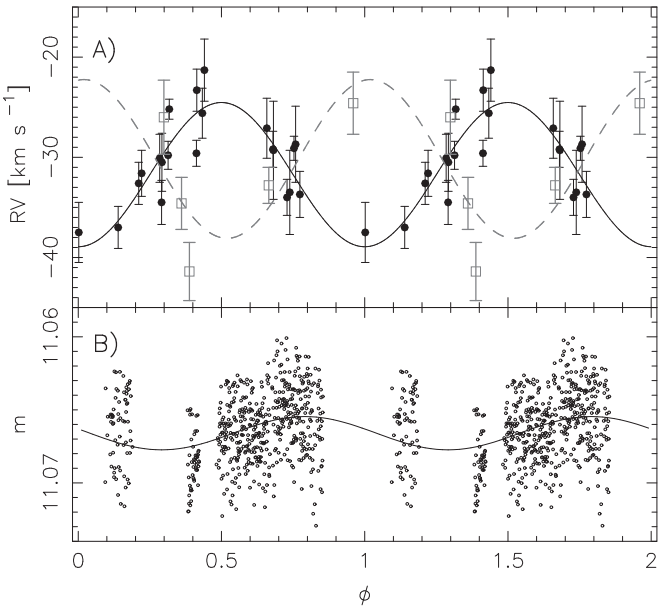

Figure 2. Upper panel: phased RV curve of M5865. The filled circles indicate the RV of the H_β line measured on high-resolution spectra. The black curve shows the orbital solution of the EHB component derived from these data. The gray squares indicate the RV of the MgIb triplet. These data were phased with the ephemeris obtained for the EHB star, and the dashed, gray curve shows their best-fit sinusoidal curve. Lower panel: photometric time series of M5865 (in instrumental V magnitudes), phased with the same ephemeris of upper panel. The best-fit sinusoidal is shown.

average of 10 fibers allocated to the sky background. Some spectra presented a wide emission feature on the red wing of the H_β line, as a result of contamination from a nearby lamp fiber. We fitted it with a Gaussian profile and removed it. We repeated the procedure varying the constraints (continuum definition and fitted data points) to estimate the uncertainty thus introduced on the RVs. This was negligible (<1 km s^{-1}) in all but two spectra, where it was of the order of 2.5 km s^{-1}. To measure the RVs, we cross-correlated (Tonry & Davis 1979) the H_β line with its wings (4840–4880 Å) with a synthetic spectrum with parameters matching those of the EHB star, drawn from the library of Munari et al. (2005). We corrected the observed RVs to heliocentric values. The spectra of about 60 hot stars were contemporarily observed by the multi-object GIRAFFE spectrograph. We estimated and removed zero-point offsets between the frames, forcing the average RV of the 40 best targets (in terms of spectral quality and measurement accuracy and showing no relevant RV variation) to be constant among the epochs (see Moni Bidin et al. 2011 for more details). We estimated the associated uncertainty from the related error-on-the-mean.

We analyzed the periodograms of the data calculated with several algorithms, such as the analysis of variance (ANOVA; Schwarzenberg-Czerny 1996, shown as an example in Figure 3), the Lomb–Scargle algorithm (Lomb 1976; Scargle 1982), the Bloomfield (1976) Fourier Analysis, the Data-Compensated Discrete Fourier Transform (Ferraz-Mello 1981), and the Fourier Analysis of Light Curves of Harris et al. (1989). A prominent peak at $P = 1.61$ days dominates all the periodograms. The corresponding phased RV curve is shown in Figure 2. This solution is robust because it is stable against the exclusion of up to five of the most uncertain measurements, and none of the secondary peaks returned an equally satisfactory

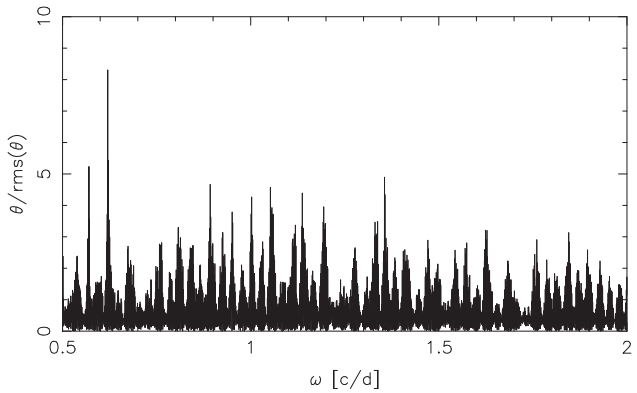

Figure 3. ANOVA periodogram of the RV data. The power spectrum is given in units of the rms.

solution in terms of rms deviation and χ^2 statistics of the fit. Despite the high significance of the RV variations (4.6σ), the semiamplitude of the RV curve (7.2 ± 0.7 km s^{-1}) is small compared to the typical variations of close EHB systems (Morales-Rueda et al. 2003). This suggests a nearly face-on orbital plane.

2.3. Visual Companion

Unfortunately, M5865 is outside the field of view of *HST* archive images. We therefore stacked our 13 best-seeing, ground-based, high spatial resolution frames in search of hints of an MS star projected along the line of sight. No physical companion should be detected, as even a wide binary system would be unresolved at the cluster distance (4.2 kpc; Harris 1996). The data were collected with MagIC at the Clay telescope at Las Campanas Observatory on 2006 May 9 with a spatial resolution of $\sim$0.″1 per pixel. The effective seeing of the composite image is 0.″41, and M5865 has exactly the same FWHM as other isolated stars in this frame. Any blended star should be closer than 0.″16, or a larger point-spread function would have been detected. M5865 is located at a distance to the center of twice the cluster half-mass radius (Harris 1996), where the crowding conditions are not severe. The density of stars within 0.′5 from M5865 in the WFI photometric catalog (Momany et al. 2002), corrected for the catalog's completeness (95% for stars with $V < 20.5$), is $\sim$0.028 stars arcmin^{-2}. Hence, the probability of a chance alignment with separation $<$0.″16 is 0.2%. As discussed in Section 2.4, the MS star is RV variable. The fraction of MS binary stars in the cluster is extremely low ($<$1% in the external regions; Milone et al. 2010), and the joint probability of having a blended MS foreground star that is also a binary is negligible ($<2 \cdot 10^{-3}$). The MS star must therefore be part of the M5865 system.

2.4. RV Variations of the Mg Triplet

We used the FORS2 spectra presented in Section 2.1 to measure and compare the RV of the H_β line and of the MgIb feature. Moni Bidin et al. (2006) showed that these data are affected by RV zero-point offsets up to 10–15 km s^{-1}, and they are suitable only for measurements of RV variations, with a precision of 3–4 km s^{-1}. We therefore measured the RV variations (ΔRV$_i$) in the spectra with respect to the first spectrum of the series, and we corrected them as detailed in Moni Bidin et al. (2006). We found RV variations of the MgIb

triplet, significant at the 3.8σ level. We then derived the absolute RV of the reference spectrum (RV_{ref}), cross-correlating it with the best-fit synthetic template used for the spectroscopic estimate of M_{MS}. The combination of ΔRV_i and RV_{ref} returned the absolute RV in each spectrum, but all these measurements were offset by the zero-point systematic of the reference spectrum. Hence, we phased the RVs of the H_β line with the ephemeris obtained in Section 2.2, then we compared them with the best-fit RV curve (black curve in Figure 2), and we minimized the χ^2 statistics to find the zero-point correction.

The third object of a hierarchical triple system must show a low-amplitude, low-frequency RV curve unrelated to the orbital period of the inner pair. The RV variations of the MgIb triplet are not compatible with this scenario because they are too large (comparable to those of the EHB star) in a temporal interval of only three days, and they are in rough antiphase with the variations of the H_β line on the same spectra. Unfortunately, the latter are not significant when compared to the large errors (Moni Bidin et al. 2006), and the measurements are too few to independently derive the periodicity of the MS star. However, when we phase the RV of the MS star with the solution previously obtained from the high-resolution spectra, we find that the best-fit sinusoidal curve is in antiphase with that of the EHB star, as shown in Figure 2. Thus, the behavior of the MgIb triplet demonstrates that the MS star is the close companion of the hotter component.

2.5. Light Variations

An EHB star with a close MS companion should show light variability (Heber et al. 2004; Geier et al. 2012). Stars deformed by tidal forces show ellipsoidal variations faster than the orbital period by a factor of two, with maxima at the phases of maximum and minimum RV. On the other hand, a star in rotationally locked orbit exhibits reflection effects on the heated hemisphere, synchronous with the orbital period and with maximum brightness at phase $\Delta\phi = 0.25$ before the minimum RV.

More than 800 frames in the V band were acquired with IMACS at the 6.5 m Baade telescope at Las Campanas Observatory, during three consecutive nights (2007 July 7–9; Catelan et al. 2008). The instrument was used at f/4.3 and binned 2×2 on the chip, for a resulting scale of $0\farcs22$ per pixel. Exposure times varied between 30 and 40 s. The weather was good during the first and third night, with an average seeing of $0\farcs7$ and $1\farcs1$, respectively. The second night was affected by strong wind, and the seeing varied between $1''$ and $1\farcs8$. We performed the photometry using standard image subtraction routines as implemented in ISIS2 (Alard & Lupton 1998; Alard 2000). We first constructed a high signal-to-noise ratio (reference) image from the 50 best-seeing images. This was convolved with a kernel to match the seeing of each input frame, with a background variable at the second order, and subtracted to it after astrometric alignment. Aperture photometry was then performed on the difference image by means of our own customized software. We masked out bad or saturated pixels, and all stars within 20 pixels from such bad features were not further considered. We fixed the aperture radius to the FWHM of the input image, and the inner and outer radius of the sky annulus to 20 and 35 pixels, respectively. We then subtracted from the light curves the median photometric zero point between each frame and the first one of the series. We considered only the brightest stars in its calculation, and we applied a 3σ clipping algorithm to exclude outliers. We eventually removed a tiny residual trend, of the order of a few mmag, forcing the average instrumental magnitude of 43 stars within $1'$ from the target to be constant among the frames. We also applied a 3σ clipping selection to clean the light curve from outliers and excluded the data points affected by large errors. We thus ended up with 585 measurements spanning a temporal interval of about 2.5 days.

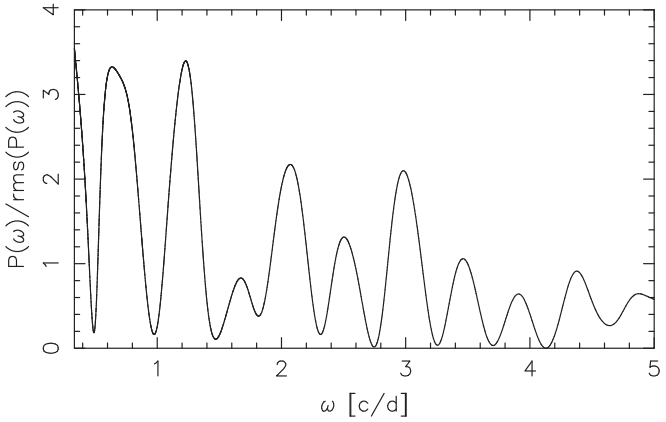

Figure 4. Lomb–Scargle periodogram of our time-series photometry of M5865. The power spectrum is given in units of the rms scatter.

The resulting periodogram is shown in Figure 4. It is characterized by wide and poorly significant peaks, as a consequence of the poor temporal sampling. However, the two dominant peaks match the orbital period and its first overtone ($P \sim 1.62$ and 0.81 days) extremely well. The corresponding light variation is tiny (of the order of 2 mmag peak-to-peak), a fact that is consistent with a high inclination of the orbital plane along the line of sight. The position of the maximum at phase $\phi = 0.75$, as shown in Figure 2, excludes ellipsoidal variations with $P \sim 0.81$ days, and it suggests that the dominant variability is due to reflection effects ($P \sim 1.61$ days) on the surface of the EHB star. This fact is new because in known systems the MS object is too cold, or too far away, to noticeably heat the EHB companion. Clearly, better time series are required to study the irradiation from this star in more detail.

3. CONCLUSIONS

Our study reveals that the close companion of the EHB star M5865 is an MS star of mass $M_{MS} \approx 0.6 M_\odot$. This discovery does not increase the low estimate of the close binary fraction in the cluster (∼4%; Moni Bidin et al. 2008) because this binary had already been identified. However, it marks a striking difference with field studies, where close binaries are very common, but M5865-like systems have never been observed.

The theoretical models predict the formation of an EHB with a close K-type, MS companion, resulting from a first common-envelope (CE) stage, although lower-mass companions are highly preferred (Han et al. 2003; Yungelson & Tutukov 2005). In an old stellar population, these systems could be more common than EHBs with a compact companion, products of a second-CE phase (Han 2008). Hence, it could not be completely surprising that the first EHB close binary studied in a GC has a K-dwarf secondary. Nevertheless, the absence in the field of such systems is harder to explain because, while

Han et al. (2003) shows that first-CE products could be a factor of two less frequent at higher metallicity, Han (2008) finds no clear decrease of the first-CE channel efficiency at younger ages. M5865-like systems have so far been overlooked in the literature due to the lack of observational counterparts, and theoretical models should study their formation mechanism in greater detail. It is also possible that they have remained undetected in the field due to selection effects such as the known "GK" bias (Han et al. 2003). In this case, the discovery of M5865 would indicate that the studies of field EHB stars are incomplete because a class of systems has so far been neglected.

C.M.B., S.V., and M.C. acknowledge support from proyectos FONDECYT regular 1150060, 1130721, and 1141141. M.C. acknowledges support by the Ministry of Economy, Development, and Tourism's Programa Iniciativa Científica Milenio, through grant IC210009, awarded to the Millennium Institute of Astrophysics (MAS) by Proyecto Basal PFB-06/2007. M.M. acknowledges support from FCT through the grant and SFRH/BDP/71230/2010.

REFERENCES

Alard, C. 2000, A&AS, 144, 363
Alard, C., & Lupton, R. H. 1998, ApJ, 503, 325
Bloomfield, P. 1976, Wiley Series in Probability and Mathematical Statistics (New York: Wiley)
Cardelli, J. A., Clayton, G. C., & Mathis, J. S. 1989, ApJ, 345, 245
Catelan, M., Prieto, G. E., Zoccali, M., et al. 2008, in ASP Conf. Ser. 392, Third Meeting on Hot Subdwarf Stars and Related Objects, ed. U. Heber, C. S. Jeffrey, & C. Koen (San Francisco, CA: ASP), 347
Chung, C., Yoon, S.-J., & Lee, Y.-W. 2011, ApJ, 740, 45
Dalessandro, E., Salaris, M., Ferraro, F. R., et al. 2011, MNRAS, 410, 694
D'Antona, F., Caloi, V., Montalbán, J., Ventura, P., & Gratton, R. 2002, A&A, 395, 69
Faulkner, J. 1972, ApJ, 173, 401
Ferraz-Mello, S. 1981, AJ, 86, 619
Geier, S., Classen, L., Brünner, P., et al. 2012, in ASP Conf. Ser. 452, Fifth Meeting on Hot Subdwarf Stars and Related Objects, ed. D. Kilkenny, C. S. Jeffrey, & C. Koen (San Francisco, CA: ASP), 153
Gray, R. O., & Corbally, C. J. 1994, AJ, 107, 742
Greggio, L., & Renzini, A. 1990, ApJ, 364, 35
Han, Z. 2008, A&A, 484, L31
Han, Z., Podsiadlowski, P., & Lynas-Gray, A. E. 2007, MNRAS, 380, 1098
Han, Z., Podsiadlowski, P., Maxted, P. F. L., & Marsh, T. R. 2003, MNRAS, 341, 669
Han, Z., Podsiadlowski, P., Maxted, P. F. L., Marsh, T. R., & Ivanova, N. 2002, MNRAS, 336, 449
Harris, A. W., Young, J. W., Bowell, E., et al. 1989, Icar, 77, 171
Harris, W. E. 1996, AJ, 112, 1487
Heber, U. 1986, A&A, 155, 33
Heber, U., Drechsel, H., Østensen, R., et al. 2004, A&A, 420, 251
Heber, U., Moehler, S., Napiwotzki, R., Thejll, P., & Green, E. M. 2002, A&A, 383, 938
Horne, K. 1986, PASP, 98, 609
Kawka, A., Vennes, S., O'Toole, S., et al. 2015, MNRAS, 450, 3514
Kurucz, R. L. 1993, CD-ROM, 13, 18 http://kurucz.harvard.edu
Lomb, N. R. 1976, Ap&SS, 39, 447
Maxted, P. F. L., Heber, U., Marsh, T. R., & North, R. C. 2011, MNRAS, 326, 1391
Milone, A. P., Piotto, G., King, I. R., et al. 2010, ApJ, 709, 1183
Momany, Y., Piotto, G., Recio-Blanco, A., et al. 2002, ApJL, 576, L65
Moni Bidin, C., Catelan, M., & Altmann, M. 2008, A&A, 480, L1
Moni Bidin, C., Moehler, S., Piotto, G., et al. 2006, A&A, 451, 499
Moni Bidin, C., Moehler, S., Piotto, G., Momany, Y., & Recio-Blanco, A. 2007, A&A, 474, 505
Moni Bidin, C., Moehler, S., Piotto, G., Momany, Y., & Recio-Blanco, A. 2009, A&A, 498, 737
Moni Bidin, C., & Piotto, G. 2010, Ap&SS, 329, 19
Moni Bidin, C., Villanova, S., Piotto, G., & Momany, Y. 2011, A&A, 528, A127
Morales-Rueda, L., Maxted, P. F. L., Marsh, T. R., North, R. C., & Heber, U. 2003, MNRAS, 338, 752
Munari, U., Sordo, R., Castelli, F., & Zwitter, T. 2005, A&A, 442, 1127
Østensen, R. H. 2006, BaltA, 15, 85
Scargle, J. D. 1982, ApJ, 263, 835
Schwarzenberg-Czerny, A. 1996, ApJL, 460, L107
Spada, F., Demarque, P., Kim, Y.-C., & Sills, A. 2013, ApJ, 776, 87
Tonry, J., & Davis, M. 1979, AJ, 84, 1511
VandenBerg, D. A., Brogaard, K., Leaman, R., & Casagrande, L. 2013, ApJ, 775, 134
Vos, J., Østensen, R. H., Németh, P., et al. 2013, A&A, 559, 54
Wade, R., Barlow, B., Liss, S., & Stark, M. 2014, in ASP. Conf. Ser. 481, Sixth Meeting on Hot Subdwarf Stars and Related Objects, ed. V. van Grootel et al. (San Francisco, CA: ASP), 311
Yungelson, L. R., & Tutukov, A. V. 2005, ARep, 49, 871